

Spectral Design of Active Mechanical and Electrical Metamaterials

H. Ronellenfisch¹ and J. Dunkel¹

¹Massachusetts Institute of Technology, Department of Mathematics, 77 Massachusetts Ave, Cambridge, MA 02139, U.S.A.
dunkel@mit.edu

Abstract – Active matter is ubiquitous in biology and becomes increasingly more important in materials science. While numerous active systems have been investigated in detail both experimentally and theoretically, general design principles for functional active materials are still lacking. Building on a recently developed linear response optimization (LRO) framework, we here demonstrate that the spectra of nonlinear active mechanical and electric circuits can be designed similarly to those of linear passive networks.

I. INTRODUCTION

Active networks model nonequilibrium systems across a wide range of scales, from the cytoskeleton [1] to traffic flow [2]. Metamaterials have similarly broad applications in engineering, physics and art, ranging from acoustics [3, 4] to sonic sculptures [5], and antennas [6, 7]. While substantial progress has been made in the design of acoustic materials [8], the functional optimization of active metamaterials has remained less explored so far. Here, we bridge this gap by applying inverse LRO design techniques [9] for discrete metamaterials to two generic classes of active networks. Specifically, we consider mechanical and electric circuits, consisting of interconnected active nodes driven by generic nonlinearities, and show that inverse bandgap-design of the underlying linear network structure can suppress active nonlinear oscillations at prescribed frequencies.

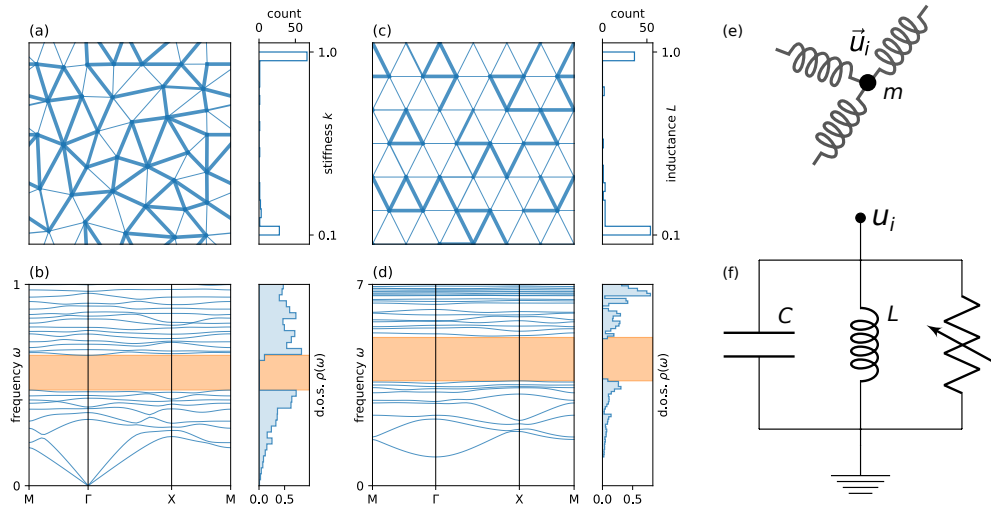


Fig. 1: Response-optimized mechanical and electrical networks. (a) Unit cell of a mechanical network on a randomized topology. Line thickness corresponds to spring stiffness. (b) Phononic band structure and density of states (d.o.s.) of the network from (a); the tuned band gap is marked in orange. (c) Unit cell of an electric LC circuit on a triangular grid. Line thickness corresponds to connecting inductance. (d) Band structure and d.o.s. of the network shown in (c); the tuned band gap is marked in orange. (e) Mechanical mass point with displacement u_i and mass m connected by three springs to the rest of the network. (f) Electrical oscillator node with voltage u_i , capacitance C , inductance L , and a nonlinear resistance.

II. MODEL AND RESULTS

As models directly amenable to inverse design [9], we consider linear second-order dynamical systems,

$$\ddot{\mathbf{u}} + D\mathbf{u} = 0, \quad (1)$$

where the vector \mathbf{u} contains the degrees of freedom and D is a positive semi-definite dynamical matrix. Specifically, we focus on two-dimensional linearized mechanical balls-and-springs networks [9] and electrical LC oscillators connected by inductors [10]. In the mechanical case, the dynamical matrix $D_{\text{mech}} = m^{-1}QKQ^\top$, where Q is the equilibrium matrix [11], K is a diagonal matrix of spring stiffnesses and m is the particle mass (Fig. 1e). In the electric circuit case, the dynamical matrix is $D_{\text{elec}} = C^{-1}(L^{-1}\mathbb{1} + EWE^\top)$, where L is the inductance of each oscillator, C is its capacitance, E is the network's oriented incidence matrix, and the diagonal matrix W contains the inverse inductances connecting the oscillators (Fig. 1f).

Both circuit systems naturally support wave propagation through phonons and electrical oscillations, respectively. In large periodic crystals, the possible modes of oscillation are described by a band structure. If this band structure is tuned, waves and oscillations can be controlled. Applying the LRO method described in Ref. [9], we designed mechanical and electric circuits by tuning spring stiffnesses K and inverse inductances W , respectively. The underlying unit cells were designed to exhibit large bandgaps around a desired frequency of oscillation (Fig. 1a–d) by minimizing the averaged linear response to forcing at frequency ω , $R(\omega) = \text{tr}(G(\omega)G(\omega)^H)$, where $\text{tr}(\cdot)$ is the matrix trace and $G(\omega) = (-\omega^2\mathbb{1} + D)^{-1}$ is the linear response matrix. We now show that this network design directly carries over from linear passive networks to non-linear active networks, where each node is endowed with the ability to convert some fuel available in the environment into motion.

A generic model for active mechanics is obtained by adding a non-linear friction force to each node [12, 13],

$$\mathbf{F}_i = -\gamma\dot{\mathbf{u}}_i + \gamma_f(1 - |\dot{\mathbf{u}}_i|^2/v^2)\dot{\mathbf{u}}_i. \quad (2)$$

Here, γ is a regular friction coefficient, the two-dimensional vectors \mathbf{u}_i and $\dot{\mathbf{u}}_i$ are the displacement and velocity of the i th node, γ_f is a measure of the nonlinearity, and v is the particle's preferred velocity. A free particle following Eq. (2) will come to rest if $\gamma > \gamma_f$ or approach the speed $|\dot{\mathbf{u}}_i| = v$ in some direction if $\gamma < \gamma_f$.

Although it is possible to obtain band structures of non-linear systems in certain cases [14], we use here an alternative approach that allows us to study the allowed modes of oscillations in a direct numerical manner. To this end, we simulated the active force Eq. (2) with the designed network dynamics Eq. (1) from Fig. 1(a) for times $t = [0, 10^4]$ from Gaussian random initial conditions and obtained time series $\mathbf{u}_i(t)$. To prevent the individual oscillators from performing collective translational motion, we fixed them in place using uniform springs of strength κ by setting $D_{\text{mech}} \rightarrow \kappa m^{-1}\mathbb{1} + D_{\text{mech}}$. To extract the active vibrational spectrum we ignored initial transients and computed the discrete Fourier transform $\hat{\mathbf{u}}_i(\omega)$ of the time series. We then averaged the Fourier spectrum over all nodes of the network to obtain the active network spectrum $\frac{1}{2}\langle |\hat{\mathbf{u}}_i|^2 \rangle_i$. The nonlinear active system shows a pronounced dip in its spectrum near the linearly designed bandgap (Fig. 2b). This suggests that the LRO-designed network structure is able to suppress nonlinear active motion at its gapped frequencies.

In a similar manner, we now consider active electrical circuits coupled to the designed network from Fig. 1(c). Following Ref. [10], we study the canonical nonlinear van der Pol relaxation oscillator [15] in the regime of weak

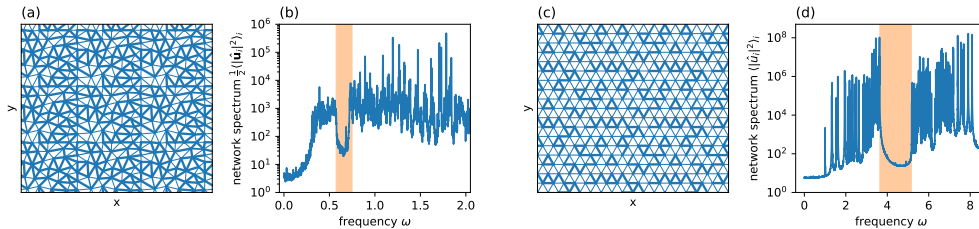


Fig. 2: Nonlinear active circuits based on the tuned unit cells from Fig. 1. (a,c) Mechanical and electrical finite-period networks consisting of 3×3 unit cells. (b,d) Temporal Fourier spectrum averaged over all active mechanical/electrical oscillators in the network. The location of the bandgaps in corresponding linear networks is marked in orange. Activity parameters for the mechanical network in (a,b) were $\kappa = 0.1, m = 1, \gamma = 0.1, \gamma_f = 0.2, v = 1$. For the electrical network in (c,d) we chose $\rho = 0.01, \varepsilon = 0.02$.

nonlinearity. Coupling the nonlinear van der Pol resistance with the network dynamics Eq. (1), we obtain the equations of motion for the dimensionless nodal voltages u_i ,

$$\ddot{u}_i + \rho \dot{u}_i - \varepsilon(1 - u_i^2)\dot{u}_i + \sum_j D_{ij}u_j = 0, \quad (3)$$

where ε is a measure of the strength of the nonlinearity and we introduced an additional resistance ρ to make formal contact with the active mechanical force Eq. (2). If $\rho < \varepsilon$, the circuit becomes active and produces self-sustained oscillations. Repeating the numerical procedure from before, we obtained spectra for the active electrical network and again find that the linearly designed bandgap carries over to the active system (Fig. 2d). This shows that the passive linear network structure can control and suppress active nonlinear dynamics in the case of electric circuits as well. Our numerical experiments suggest, however, that in the van der Pol network, this is only possible for weak nonlinearity ($\varepsilon \lesssim 0.05$) whereas the mechanical network can control much larger nonlinear active forces.

III. CONCLUSIONS

We have demonstrated that both linear mechanical and electrical networks can be inversely designed using LRO optimization methods [9], and that designed spectral gaps and accompanying suppression of motion at certain frequencies carry over to nonlinear active networks. The networks considered above are prototypical examples of active metamaterials, and we expect that inverse design of such materials will find fruitful applications in engineering, physics, and biology.

REFERENCES

- [1] C. P. Broedersz and F. C. MacKintosh. Modeling semiflexible polymer networks. *Reviews of Modern Physics*, 86(3):995–1036, jul 2014.
- [2] G. M. Coclite, M. Garavello, and B. Piccoli. Traffic Flow on a Road Network. *SIAM Journal on Mathematical Analysis*, 36(6):1862–1886, jan 2005.
- [3] P. A. Deymier, editor. *Acoustic Metamaterials and Phononic Crystals*, volume 173 of *Springer Series in Solid-State Sciences*. Springer, Berlin, 2013.
- [4] S. A. Cummer, J. Christensen, and A. Alù. Controlling sound with acoustic metamaterials. *Nature Reviews Materials*, 1(3):16001, feb 2016.
- [5] R. Martínez-Sala, J. Sancho, J. V. Sánchez, V. Gómez, J. Llinares, and F. Meseguer. Sound attenuation by sculpture. *Nature*, 378(6554):241–241, nov 1995.
- [6] J. C. Soric, R. Fleury, A. Monti, A. Toscano, F. Bilotti, and A. Alù. Controlling Scattering and Absorption With Metamaterial Covers. *IEEE Transactions on Antennas and Propagation*, 62(8):4220–4229, aug 2014.
- [7] G. Minatti, M. Faenzi, E. Martini, F. Caminita, P. De Vita, D. Gonzalez-Ovejero, M. Sabbadini, and S. Maci. Modulated Metasurface Antennas for Space: Synthesis, Analysis and Realizations. *IEEE Transactions on Antennas and Propagation*, 63(4):1288–1300, apr 2015.
- [8] M. P. Bendsoe and O. Sigmund. *Topology optimization: theory, methods, and applications*. Springer, Berlin, 2003.
- [9] H. Ronellenfitsch, N. Stoop, J. Yu, A. Forrow, and J. Dunkel. Inverse design of discrete mechanical metamaterials. *Physical Review Materials*, 3(9):095201, sep 2019.
- [10] T. Kotwal, H. Ronellenfitsch, F. Moseley, A. Stegmaier, R. Thomale, and J. Dunkel. Active topoelectrical circuits. arXiv:1903.10130.
- [11] T. C. Lubensky, C. L. Kane, Xiaoming Mao, Anton Souslov, and Kai Sun. Phonons and elasticity in critically coordinated lattices. *Reports on Progress in Physics*, 78(7):073901, jun 2015.
- [12] F. G. Woodhouse, H. Ronellenfitsch, and J. Dunkel. Autonomous actuation of zero modes in mechanical networks far from equilibrium. *Physical Review Letters*, 121(17):178001, may 2018.
- [13] P. Romanczuk, M. Bär, W. Ebeling, B. Lindner, and L. Schimansky-Geier. Active Brownian particles. *The European Physical Journal Special Topics*, 202(1):1–162, mar 2012.
- [14] R. K. Nariseti, M. Ruzzene, and M. J. Leamy. A Perturbation Approach for Analyzing Dispersion and Group Velocities in Two-Dimensional Nonlinear Periodic Lattices. *Journal of Vibration and Acoustics*, 133(6):061020, dec 2011.
- [15] B. van der Pol. On “relaxation-oscillations”. *The London, Edinburgh, and Dublin Philosophical Magazine and Journal of Science*, 2(11):978–992, nov 1926.